Microsc. Microanal. 8 (Suppl 2), 2002
10.1017/S1431927602100791

On the Control of Atomic Clustering, Segregation and Partitioning: Nanoscale Materials Technology

S.P. Ringer

Australian Key Centre for Microscopy & Microanalysis, The University of Sydney, NSW, 2006, Australia

This work summarises the application of microscopy and microanalysis at high resolution to study atomic clustering, segregation and partitioning in selected materials developments. Such studies are increasingly necessary in order to understand structure-property relationships in nanoscale materials technology. Whilst the structure, orientation and, in many cases, the composition of primary and secondary phases including nanoscale precipitation of GP zones and other phases are readily observed and measured using analytical transmission electron microscopy (TEM), clear observation of clustering, segregation and partitioning requires more advanced approaches. In this work, TEM, STEM microanalysis and three-dimensional atom probe (3DAP) to observe these effects in a selection of scientific alloys.

A series of Al-2.5Cu-xMg alloys have been studied, where $0.1<x<1.7$ Mg (wt. %). It was shown that the well-known rapid hardening effect in this system requires a threshold of ~0.5 Mg. The behaviour of the quenched-in defect structure upon ageing is shown to be distinctly different for alloys containing $x \geq 0.5$ Mg in that the rate and extent of growth of dislocation loops was much higher in these higher Mg containing alloys (Fig. 1). We have correlated this to the vacancy content and solute-vacancy interactions. On the basis of measurements of the vacancy-loop characteristics from TEM images such as Fig. 1, we have calculated that concentration of Mg atoms per nm on the average dislocation loop may be as much as 8-10 times higher in the 0.5Mg alloy compared to the 0.2 alloy.

The effect of trace additions (~0.01 at. %) of Cd on the enhanced precipitation of θ' (Al_2Cu, *I4/mcm*, *a*=0.404 nm and *c*=0.580 nm) has been studied in a set of Al-4Cu (-0.3Mg-0.5Cd) (wt. %) alloys. The effect was confirmed in all Cd-containing alloys and in the Al-Cu-Cd alloy, elemental Cd precipitates were detected uniformly throughout the matrix and attached to θ'. On the other hand, co-clustering of Cd-Mg atoms was detected using 3DAP in the Al-Cu-Mg-Cd alloy during the early stages of ageing. This clustering was followed by the precipitation of a Cd-Mg rich precipitate, which was observed in association with all strengthening phases. Furthermore, it was shown that all of the Cd-bearing phases are able to nucleate the θ' and concomitantly, that the θ' is able to nucleate the Cd-bearing phases.

Finally, the crystallisation of nanocrystalline α-Fe in $Fe_{89-x}Zr_7B_3Cu_1Ge_x$ alloys has been studied using a dedicated VG STEM. Although the T_C of the Ge-free alloy is below room temperature, it is enhanced to 360 K at $x = 5$, indicating that Ge is effective in enhancing the exchange stiffness of Fe-rich amorphous Fe-Zr-B. These results indicate that Ge-induced magnetic softening in $Fe_{89-x}Zr_7B_3Cu_1Ge_x$ is due to the preferential enrichment of Ge into the residual amorphous phase which results in an enhancement of the exchange stiffness in the intergranular region.

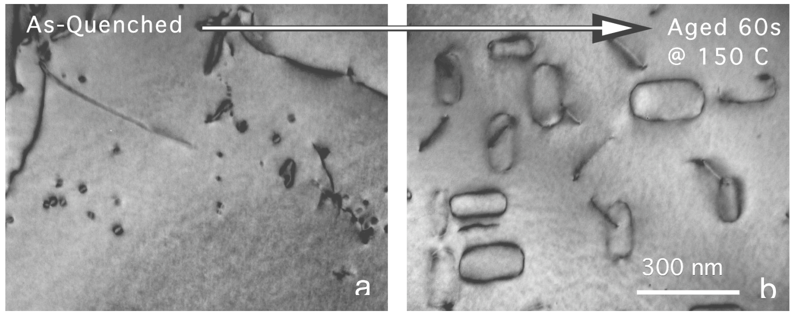

FIG. 1. BF TEM images recorded near <001>$_{□}$ of the defect structures of Al-2.5Cu-0.5Mg (wt. %) after quenching (a) and after ageing for 60 sec at 150°C (b). Approximately 60% of the hardening reaction occurs in the first few seconds of ageing.

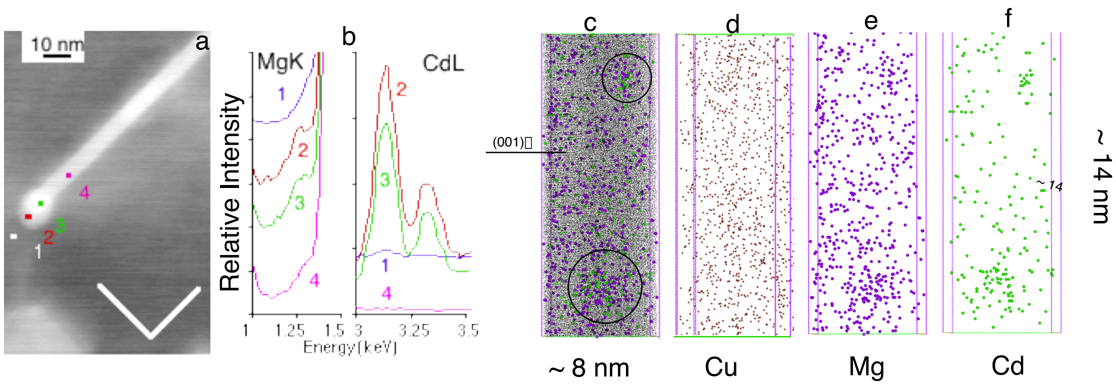

FIG. 2. (a) <001>$_{□}$ DF STEM image of typical □' in the peak hardness microstructure of the Al-Cu-Mg-Cd alloy with the Mg and Cd EDXS profile from the points 1-4, indicated. The cube traces are marked in (a). (c-f): 3DAP elemental mapping of Al-Cu-Mg-Cd alloy aged at 200 °C, 15 min showing the presence of two clusters. Maps for (c) all atoms (d) Cu (e) Mg and (f) Cd atoms.

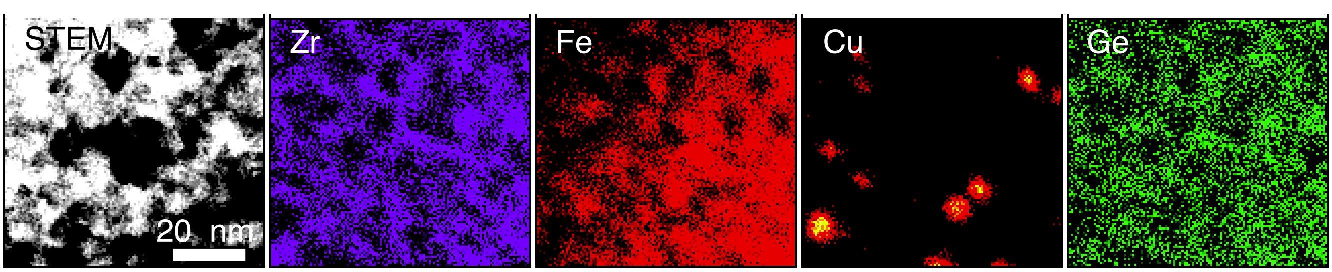

FIG. 3. BF STEM and chemical maps from $Fe_{86}Zr_7B_3Ge_3Cu_1$ following annealing for 1 h at 550 °C. The Ge is partitioned into the residual amorphous and is rejected from the nanocrystalline □-Fe grains. Clusters of Cu were also detected. A probe size of ca. 1 nm was used.

This research was supported by the Australian Research Council. Contributions and valuable discussions from B. T. Sofyan, G. B. Winkelman and K. Suzuki from Monash University are gratefully acknowledged.